University of Groningen

Long-distance facilitation of coastal ecosystem structure and resilience

Wang, Bo; Zhang, Kang; Liu, Quan Xing; He, Qiang; van de Koppel, Johan; Teng, Shuqing N.; Miao, Xinyu; Liu, Maosong; Bertness, Mark D.; Xu, Chi

IMPORTANT NOTE: You are advised to consult the publisher's version (publisher's PDF) if you wish to cite from it. Please check the document version below.

Document Version
Publisher's PDF, also known as Version of record

Link to publication in University of Groningen/UMCG research database

Long-distance facilitation of coastal ecosystem structure and resilience

Bo Wang (王博)[a,1] 🅘, Kang Zhang (张康)[b,1] 🅘, Quan-Xing Liu (刘权兴)[b,c,2] 🅘, Qiang He[d], Johan van de Koppel[e,f] 🅘, Shuqing N. Teng[a], Xinyu Miao[a], Maosong Liu[a] 🅘, Mark D. Bertness[g], and Chi Xu (徐驰)[a,2] 🅘

Biotic interactions that hierarchically organize ecosystems by driving ecological and evolutionary processes across spatial scales are ubiquitous in our biosphere. Biotic interactions have been extensively studied at local and global scales, but how long-distance, cross-ecosystem interactions at intermediate landscape scales influence the structure, function, and resilience of ecological systems remains poorly understood. We used remote sensing, modeling, and field data to test the hypothesis that the long-distance impact of an invasive species dramatically affects one of the largest tidal flat ecosystems in East Asia. We found that the invasion of exotic cordgrass *Spartina alterniflora* can produce long-distance effects on native species up to 10 km away, driving decadal coastal ecosystem transitions. The invasive cordgrass at low elevations facilitated the expansion of the native reed *Phragmites australis* at high elevations, leading to the massive loss and reduced resilience of the iconic *Suaeda salsa* "Red Beach" marshes at intermediate elevations, largely as a consequence of reduced soil salinity across the landscape. Our results illustrate the complex role that long-distance interactions can play in shaping landscape structure and ecosystem resilience and in bridging the gap between local and global biotic interactions.

biological invasion | biotic interaction | long-distance interaction | resilience | coastal saltmarsh

G. E. Hutchinson's question "Why are there so many kinds of animals?" has sparked decades of exploring the origins of biodiversity (1). Many ecologists including Hutchison have suggested that the answer to this fundamental question largely hinges on biotic interactions (2–4). Indeed, the ways in which organisms interact with one another may be just as diverse as the number of interacting organisms. Biotic interactions arise inevitably when plants, animals, and microbes coexist in close proximity, sharing the same resources, responding to the same stresses, or foraging on one another, but what if organisms are located far away from each other?

The answer is counterintuitive: Strong interactions can occur between sessile organisms even if they are separated by long distances, far beyond the spatial domains of local coexistence typical of submeter or meter levels. The ecological–evolutionary processes that have shaped our biosphere are an "extreme" case of biotic interactions operating at global scales. Cyanobacteria production of oxygen, for example, drove the Great Oxygenation Event about 2.4 billion y ago, leading to oxidative metabolism and the evolution of eukaryotic plants and animals (5). Synthesizing these lines of evidence may give rise to understanding how biotic interactions operate across spatial scales from local to global. This idea, however, is challenged by a paucity of evidence documenting biotic interactions operating at intermediate landscape scales.

Examples of landscape-scale biotic interactions are sparse relative to local and global examples. Evidence includes competition for soil water between plants growing in spatially separate patches of dryland vegetation (6, 7) and facilitation between plant species at different elevations across coastal landscapes (8). These "long-distance interactions" (9) have been suggested to occur only in a handful of systems. Mounting empirical evidence, however, is emerging in a number of ecosystems [e.g., mussel beds and cobble beaches (10, 11)] where long-distance interactions shape ecosystem structure, function, and resilience, suggesting that they may play a more fundamental and widespread role in shaping ecosystems than previously thought. Long-distance interactions have generated theoretical advances in ecology, as reflected in spatial self-organization (12–14) and metaecosystem theory (15), and have critical implications for ecosystem conservation and restoration (9). Understanding long-distance interactions may also elucidate general relationships between the small-spatial-scale biotic interactions studied by experimental community ecologists and the feedbacks between the biota and environmental processes that drive the dynamics of ecosystems at regional and global scales studied by modelers and ecosystem ecologists.

Significance

"Red Beach" ecosystems along the Yellow Sea coastline are biodiversity hotspots critical for migratory shorebirds of the East Asian–Australasian Flyway. Satellite images show that these ecosystems have been shrinking markedly in recent decades. The reasons for this loss are unknown. Here, we reveal a landscape-scale biotic interaction driven by the destructive effect of invasive cordgrass on native coastal saltmarsh ecosystems that has progressively emerged over the past four decades. In contrast to previous studies showing positive effects of long-distance interactions, our study demonstrates that this negative interaction operating over 10 km is leading to the extinction of the "Red Beach" ecosystem and will dramatically impact ecosystem resilience to sea-level rise in the coming decades.

[1]B.W. and K.Z. contributed equally to this work.

[2]To whom correspondence may be addressed. Email: qxliu@sklec.ecnu.edu.cn or xuchi@nju.edu.cn.

Coastal ecosystems commonly have striking biotic spatial organization dominated by foundation species conducive to revealing long-distance interactions. A common class of coastal long-distance interactions is mediated by mobile consumers that migrate between spatially disjoined foundation species habitats, mediating their interactions. Interactions also commonly occur between sessile organisms over long distances when they compete for moving resources, such as sediment nutrients for seagrass and mangroves, or planktonic food for mussels and cockles or when they are facilitated/interfered by moving non-living substances (16). Indirect long-distance interactions can also arise when the presence of sessile organisms modifies physical environments, influencing the organisms that live there. This is found on cobble beaches and mudflats, where cordgrass at lower elevations can facilitate wave-vulnerable forbs at higher elevations by reducing wave impacts (8, 11). Similar long-distance interactions mediated by environmental modifications have been documented across coastal landscapes composed of two or more distinct, spatially mixed foundation species such as mussel and cockle beds, seagrass meadows, and oyster and coral reefs (9).

While examples of long-distance interactions are accumulating, our understanding of their consequences and functioning remains limited. Importantly, even if long-distance interactions are omnipresent, we do not know if and to what extent they are strong enough to impact ecosystem persistence and resilience. It has been speculated that long-distance interactions can enhance ecosystem resilience (17, 18), based on the documented positive role of long-distance interactions in the maintenance of biodiversity and provisioning of ecosystem services (9). However, this cannot rule out the possibility that long-distance interactions can also have negative effects on ecosystem persistence and resilience. These effects are particularly relevant with Anthropocene accelerating climate change and human activities but remain largely unknown.

Here, we use remote sensing, modeling, and field data to examine the hypothesis that a novel long-distance interaction drove a decadal landscape transition along a Chinese coastline. The coastal landscape examined is the salt marsh ecosystem of the Yellow Sea. Historically this ecosystem had striking vertical intertidal zonation. The low intertidal habitat was dominated by unvegetated mudflats. The middle marsh habitat, hypersaline due to the evaporative accumulation of salt, was dominated vegetatively by the red native succulent *Suaeda salsa* and other salt-tolerant plants that live in this physically harsh habitat as a competitive refuge. The high marsh habitat was dominated by a dense monospecific zone of the native reed *Phragmites australis*. Of these zones, the middle marsh *Suaeda* zone is ecologically and economically the most valuable. Expansive red *Suaeda* marshes are culturally valued as a tourist attraction (19), have a high diversity of native plants and animals (20, 21), and are critical for migratory shorebirds of the East Asian–Australasian Flyway (22, 23). For example, they support ∼500 to 1,100 individuals of red crowned crane (*Grus japonensis*) annually, accounting for ∼15 to 30% of the global population of this protected species (24). However, these ecosystems have been shrinking over the last few decades (25, 26) for reasons that remain unknown.

In this paper we show that the loss of the ecologically and economically valuable *Suaeda* red marsh zone is attributed to a cross-ecosystem interaction occurring at distances up to 10 km, triggered by the invasion of an alien cordgrass species *Spartina alterniflora* since the 1990s and its indirect impacts on marsh sedimentation and salinity. We tested the hypothesis that the invasion of *Spartina* as an important ecosystem engineer altered landscape-scale soil salinity through reduced tidal inundation, cascading to influence the competition between *P. australis* and *S. salsa*. The direct ecological impacts of cordgrass invasion on local scales has long been recognized, but their indirect impacts at larger spatial and temporal scales began to emerge only recently (26). We used a simple model that reflected the remotely sensed system dynamics to show how the long-distance effects of cordgrass could play a destructive role in inducing loss of native *Suaeda* habitats and how coastal resilience to sea-level rise could be shaped by this landscape-scale biotic interaction.

Results and Discussion

Remotely Sensed Landscape Transitions. We analyzed a time series of Landsat images at 30-m resolution to quantify landscape dynamics from 1982 to 2020. Our analysis shows that before the invasion of cordgrass the native coastal landscape had distinctive zonation characterized by bare mudflats at low elevations and the reed-dominated vegetation at high elevations, separated by extensive saltmarsh flats dominated by the succulent forb *S. salsa* (Fig. 1). Following the 1982 introduction of the alien cordgrass *S. alterniflora*, however, the years after 1990 have been characterized by accelerated vegetation transitions across the landscape. Following exotic cordgrass invasion, cordgrass and reeds have both continuously increased in vegetation cover until the present, while the native *Suaeda* forb zone has dramatically declined in cover since ∼2005 (Fig. 1).

Interestingly, while cordgrass appears to have triggered this landscape change, most habitats undergoing *Suaeda* loss were transformed into a state dominated by reeds rather than cordgrass (Fig. 1 and *SI Appendix*, Table S2). This is also clearly reflected by our "spatial niche" analysis of the one-dimensional (along the land–sea gradient) distribution ranges of the three dominant species (see *Materials and Methods* and Fig. 1*F*). The core distribution range (measured by the breadth of the "spatial niche") of the cordgrass exhibited an abrupt increase during early colonization, followed by saturation (see Fig. 3*B*). This plateau-shaped temporal pattern indicates that cordgrass, upon successful invasion (colonization), occupied a relatively stable "spatial niche" that was originally bare mudflat. Yet, it dramatically affected the landscape landward.

Mechanism of Long-Distance Interaction. While cordgrass invasion has not directly displaced and transformed the native forb vegetation zone dominated by *Suaeda*, cordgrass is likely responsible for the transition of forb to reed habitats that occurred kilometers away from the cordgrass zone. This hypothesis is based on a mechanism of indirect long-distance interaction (Fig. 2). Establishment of cordgrass at the low-elevation mudflats modifies water flow, increasing the deposition of sediment and enhancing the accumulation of peat substrate (27). This elevates the landscape in the cordgrass zone and is the primary mechanism underlying the biogenic deposition of salt marsh habitats. The presence of a hypersaline zone and the halophyte *Suaeda* is strongly dependent on tidally driven episodic accumulation of salt killing its competitors. Monthly spring high tide inundation of saltwater is key to maintaining the high salt content of the hypersaline *Suaeda* habitat at intermediate marsh elevations. At lower elevations daily tidal inundation limits the buildup of salinity by flushing the marsh surface with ambient saltwater, washing away salt that accumulated due to the evaporation of surface sediments. At intermediate elevations only flooded monthly by spring tides, hypersaline sediment develops evaporative water loss due to limited tidal flooding.
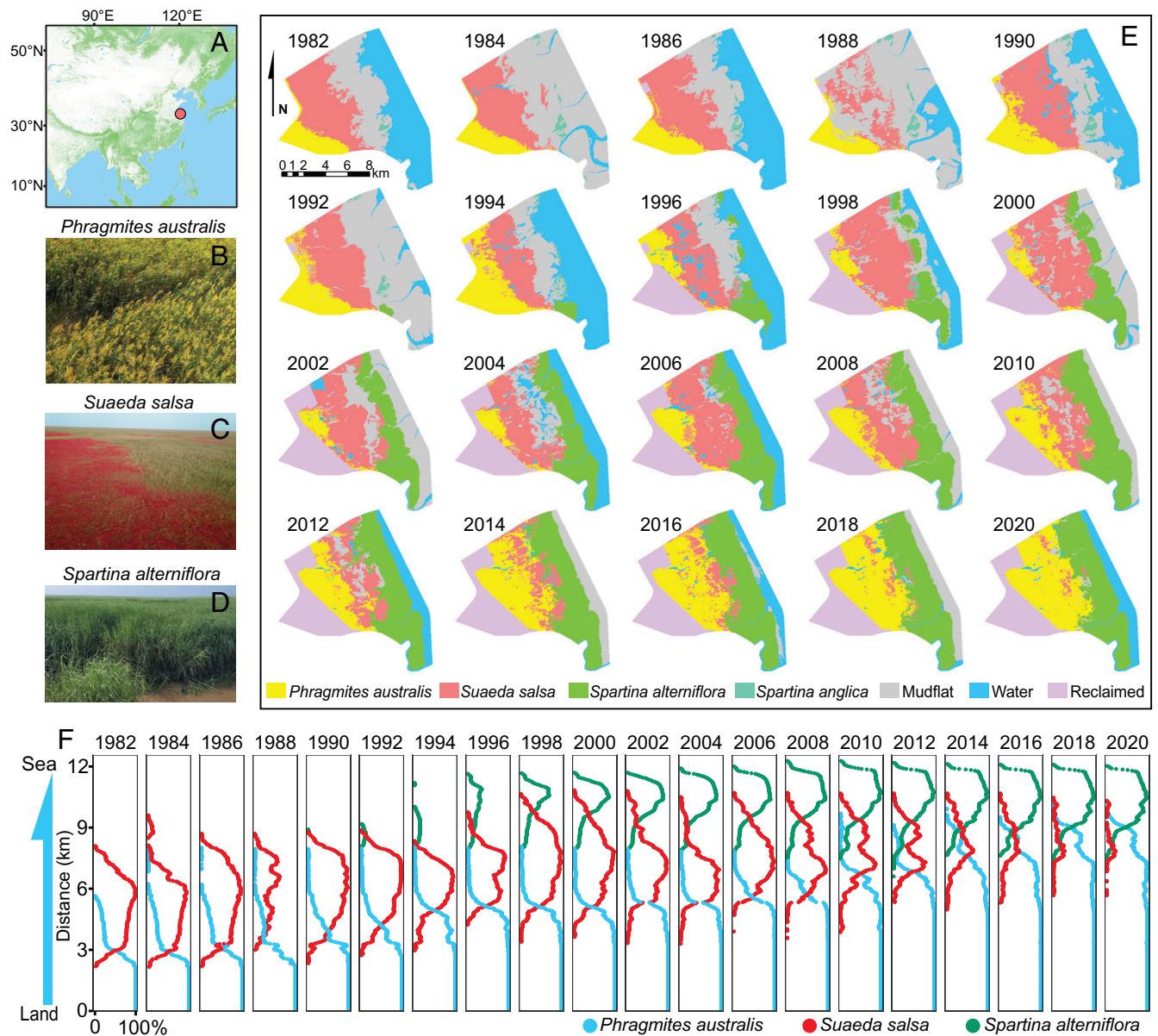
Fig. 1. Remotely sensed landscape change in the studied coastal region during 1982 to 2020. (A) Location of the study area. (B–D) Photos of vegetation dominated by *P. australis*, *S. salsa*, and *S. alterniflora*. (E) Maps of vegetation distribution in the study area. (F) Percent covers of the vegetation along the one-dimensional spatial gradient from land to sea. Note that the landscape changes are illustrated on a biannual basis here (E and F), whereas data analyses are performed on an annual basis (see *SI Appendix*, Fig. S2 for a complete illustration).

At higher elevations decreasing inundation by tides (28), precipitation and surface and subsurface water flow limit salt accumulation and promote desalinization of marsh sediments. Desalination at intermediate-high elevations can facilitate the expansion of salt-intolerant but competitively dominant reeds. A critical consequence of this long-distance facilitative effect is that suitable habitat for reeds is expanded seaward, where they outcompete and replace *Suaeda*.

This long-distance hypothesis is supported by the long-term data of sediment, elevation, and soil salinity revealing the changes before and after the *Spartina* invasion (29–31). The invasion triggered a clear building process characterized by enhanced sedimentation by *Spartina* and significant increases of elevation at the local scale (Fig. 3C and *SI Appendix*, Fig. S3). In contrast, elevation did not show apparent change in the *Suaeda* and *Phragmites* zones during this period (Fig. 3C), suggesting that elevation per se may not be the key factor

responsible for the observed transition. Also, sediment composition changed from a sand- to silt-dominated state in the *Spartina* zone due to *Spartina*'s strong ability capturing fine-grained sediments. In the *Spartina* zone, a sharp increase of silt fraction was detected around the 60-cm sediment layer, plausibly corresponding to the establishment of *Spartina* (Fig. 3C, IV). In contrast, such an increase was detected around the depth of 30 cm in the *Suaeda* zones, suggesting a time lag of sedimentation change relative to the *Spartina* zone. The increment of sediment surface elevation in the *Spartina* zone will increasingly block low-level sea waters, leading to progressively shorter inundation and lower salt input from tides to the *Phragmites* and *Suaeda* zones landward. Long-term monitoring of inundation time has not been implemented in previous studies, but we find a clear trend of declining salinity in the *Suaeda* zone, starting around 2005 (Fig. 3G). This desalination trend is in strong agreement with the landscape vegetation transitions.
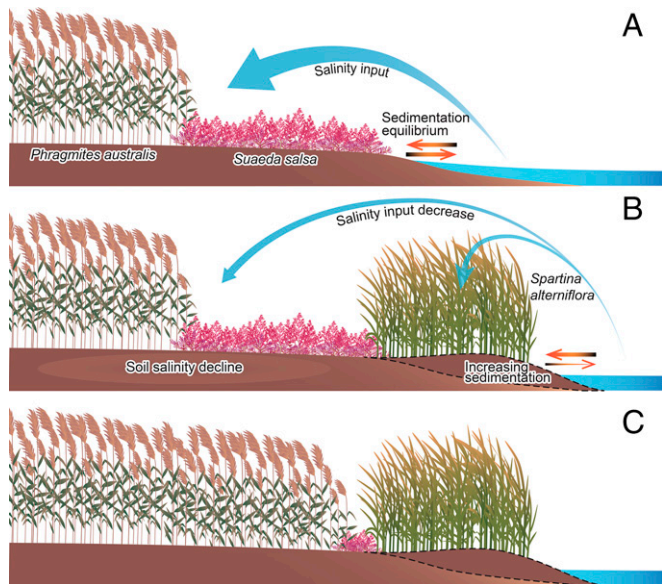
Fig. 2. Schematic illustration of the long-distance interaction triggered by *Spartina* invasion. (*A*) Sedimentation-erosion equilibrium and salinity input from tidal water ensure the persistence of the extensive red *Suaeda* salt-marsh before the *Spartina* invasion. (*B*) The invasion of *Spartina* triggers a building process characterized by enhanced sedimentation and increased elevation at the local scale. At a larger scale across the landscape at higher elevations behind the *Spartina* zone, the elevated low tidal zone produces a blocking effect, resulting in reduced salinity input from tidal water and declined soil salinity due to shorter inundation, in turn facilitating the expansion of *Phragmites*. (*C*) This long-distance effect of *Spartina* eventually leads to the massive loss of *Suaeda*, as replaced by *Phragmites*.

Putting these spatiotemporal patterns together suggests that the *Spartina* invasion was associated with the time lags observed in transitions of sediment composition, salinity, and vegetation type.

Modeling Long-Distance Interaction. Since this hypothesized mechanism would be difficult to test with manipulative experiments, due to the large spatiotemporal nature of the observed landscape vegetation shift, we developed a simple model to examine if the long-distance interaction could explain the observed vegetation dynamics. We used the 1990 landscape configuration as a starting point and modeled the percent cover of *Spartina*, *Suaeda*, and *Phragmites* across the land–sea gradient. The dynamics of vegetation cover are determined by four critical ecological processes: 1) spatial diffusion, 2) logistic growth, 3) interspecific competition, and 4) long-distance interactions. We built on the Lotka–Volterra competition model to incorporate a spatial diffusion term and a long-distance interaction mechanism. The long-distance effect of cordgrass is modeled as a process of increasing elevation in the low-tide zone and reduced tidal water inundation, which consequently reduces soil salt content on the tidal flat, thereby changing the interspecific competition coefficient between *Suaeda* and *Phragmites* (see *SI Appendix*, section S1 for model details). Competitive interactions can be mediated by resource and/or stress. Here, salt stress is considered the primary factor determining the competitive interactions in our saltmarsh ecosystems.

Despite its simplicity, the model captured the observed system dynamics surprisingly well. From a spatial perspective, our model captured that the traveling front of *Phragmites* migrated seaward to compress the *Suaeda* zone, whereas the *Spartina* zone was spatially stable (Fig. 4*A*). We found good fits between modeled and observed soil salinity, vegetation cover, and spatial niche across the decadal study period (Fig. 4 *B–D*, *SI Appendix*, Fig. S4 and Movie S1). Particularly, the time lag of ~5 y between

the decline of the *Suaeda* spatial niche (starting around 2000) and the expansion of the cordgrass spatial niche (starting around 1995) are captured by the model that reflects the relatively slow salinity change after the successful *Spartina* invasion (Fig. 4*D*). An important finding is that even a mild long-distance interaction would eventually lead to *Suaeda* zone extinction (*SI Appendix*, Fig. S6*E*). Although our simple model may serve as a starting point for testing the effect of the long-distance interaction, further incorporating mechanisms of sediment deposition and hydrodynamics with relevant validation data (if available) may help to look into the system behavior in a more realistic way. While our theoretical model could not provide a rigorous test of the mechanisms, it demonstrates the inferred long-distance interaction mechanism is indeed possible to give rise to the observed pattern.

The Shaping Role of Long-Distance Interaction. If our model reflects the mechanisms underlying the observed system dynamics, it can serve as a tool to infer the role of the long-distance interactions in shaping coastal landscapes. The model predicts that in the absence of long-distance interaction/facilitation of reeds, the system would converge to an equilibrium characterized by the stable coexistence of three vegetation types across the landscape. Following cordgrass invasion, a two-vegetation (dominated by reeds and cordgrass) state emerges due to strong long-distance facilitation between cordgrass and reeds (Fig. 5), where salt stress plays a mediating role. Long-distance interactions thus likely play a critical role in shaping both physical conditions and habitat zonation along this coastal landscape. The striking spatial structure or zonation of the new landscape state is not simply a reflection of environmental or physical factors but rather largely results from biotic interactions operating along physical gradients (32, 33).

Long-distance interactions could underlie a dramatic change of the resilience of the coastal vegetation subjected to accelerated sea-level rise. In the original state, salinity increases as a primary effect of sea-level rise (34), and the *Suaeda* marsh zone can easily adapt to sea-level rise by moving landward, provided that sufficient space is available. In contrast, with strong long-distance interactions following cordgrass invasion and the loss of the *Suaeda* marsh zone, sea-level rise will be met by a much more persistent zone of cordgrass that will adapt by increasing sedimentation both within the cordgrass zone itself as well as in the reed habitat in its wake. Hence, cordgrass invasion fundamentally changes the resilience of coastal ecosystems, from one defined by zonation that can adapt to sea-level rise by moving landward to a much more resistant ecosystem where sedimentation generates marsh expansion but becomes increasingly vulnerable at its exposed edge if the elevated habitat becomes more vulnerable to wave attack (35). It is also likely that the *Suaeda* marsh zone will gain resilience from sea-level rise due to elevated sediment salinity, a scenario predicted by the model (Fig. 6*A*). In the long term, the *Suaeda* marsh zone on the verge of regional extinction may be rescued by sea-level rise at sufficiently rapid rates (Fig. 6*B* and *SI Appendix*, Fig. S7). Thus, the fate of the *Suaeda* marshes and the ecosystem services they provide remain uncertain over the next century and largely depend on the speed of sea-level rise.

A basic insight from this research is that long-distance interactions can drive cross-ecosystem spatial self-organization at a large scale. At within-ecosystem spatial scales, spatial self-organization results from a coupled short-range positive and long-range negative feedback (13), giving rise to regular spatial patterning in many ecosystems (ref. 36, but see ref. 11). The long-distance
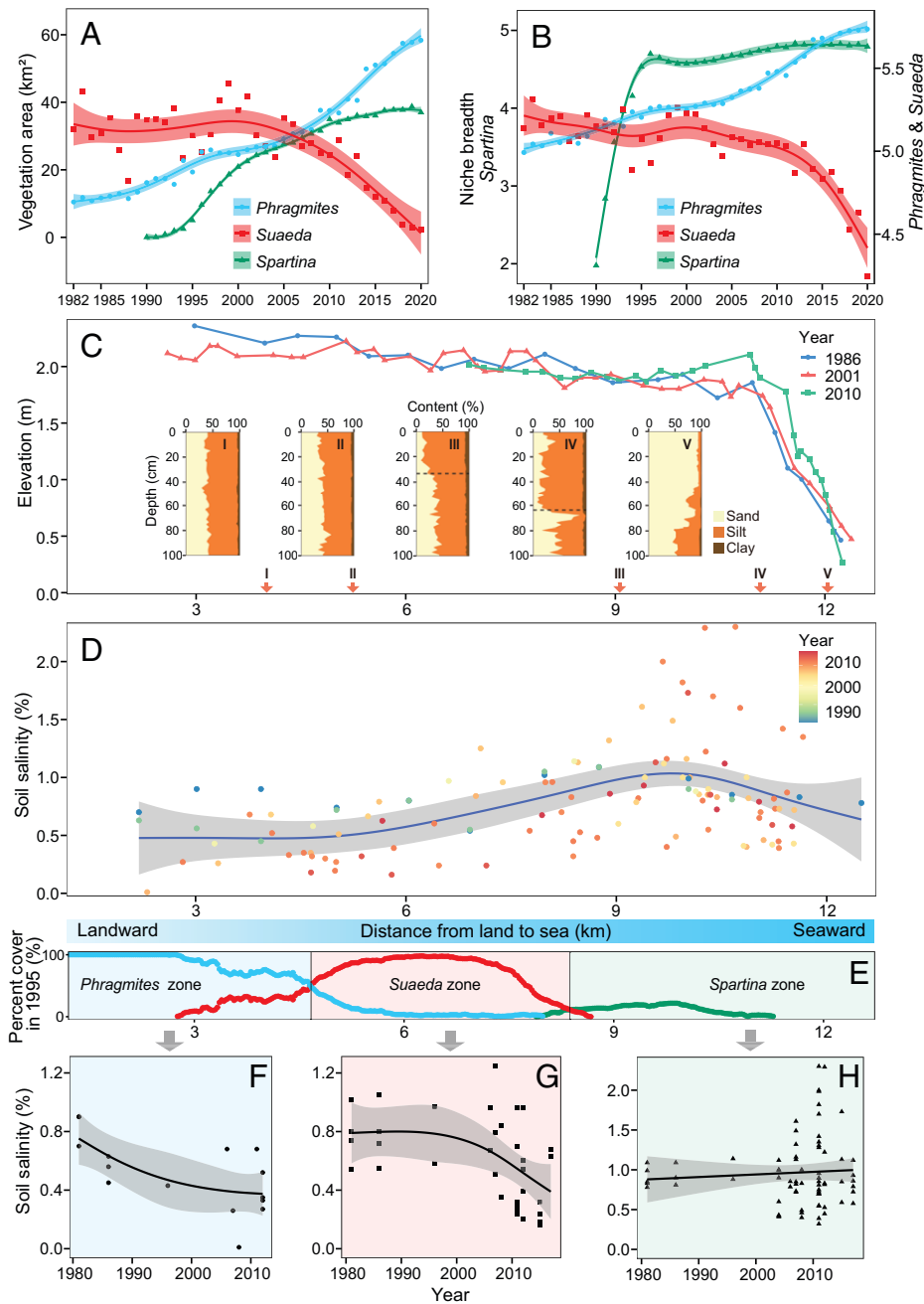
Fig. 3. The spatiotemporal patterns of elevation, soil and vegetation. (*A*) Time series of vegetation area show increasing trends of *Phragmites* (blue) and *Spartina* (green) but an abruptly declining trend of *Suaeda* (red). (*B*) Time series of the breadths of the "spatial niches" along the spatial gradient from land to sea show that the core distribution range of *Spartina* (green) increased abruptly before ~1995, followed by a saturation trend afterward. The time series of *Phragmites* (blue) and *Suaeda* (red) show piecewise trends with a consistent turning point around 2005. (*C*) Elevation data show clear increases of elevation after the successful invasion of *Spartina* (2001 to 2010) in the *Spartina* zone but not in the *Suaeda* zone. The five inset panels show the vertical distribution of sediment composition in terms of fractions of sand, silt and clay (measured in 2007, locations labeled as I to V). The dashed lines indicate the turning points of the vertical distribution patterns of % silt (fine sediments), detected using a break point analysis. The elevation and sediment composition data were obtained from refs. 30 and 31. (*D*) Soil salinity generally shows a humped pattern along the spatial gradient from land to sea, peaked in the cordgrass zone. Point color indicates the year when salinity was measured. (*E*) The studied landscape can be separated into three distinctive vegetation zones on the basis of vegetation distribution along the land–sea spatial gradient in 1995. The intersection points of the percent cover curves are used to identify the boundaries of the vegetation zones. (*F–H*) The temporal trends of soil salinity in the above-mentioned vegetation zones separately show different patterns: a linear-like decreasing trend in the *Phragmites* zone (*F*), an abruptly decreasing trend after ~2005 in the *Suaeda* zone (*G*), and a slightly increasing trend in the *Spartina* zone (*H*). Note that the y axis range in *H* is different from in *F* and *G*. The trends in *A*, *B*, *D*, and *F–H* are fitted using generalized additive models with 95% CIs.

interactions studied here would give rise to distinct spatial organization of different ecosystems at larger spatial scales. These mechanisms may interact to generate hierarchical self-organization across spatial scales (37). Long-distance interactions not only can have unexpected ecological impacts on community structure and organization but acting over long distances and long-time spans, they can also have evolutionary consequences by impacting isolation by

distance. The evolutionary consequences of global-scale biotic interactions has been recognized as important in life and earth sciences (37). Landscape, long-distance interactions may also create this potential.

Our study has important implications for how coastal systems in general respond to disturbances. Droughts can have important consequences for the coasts of eastern China. Long-distance
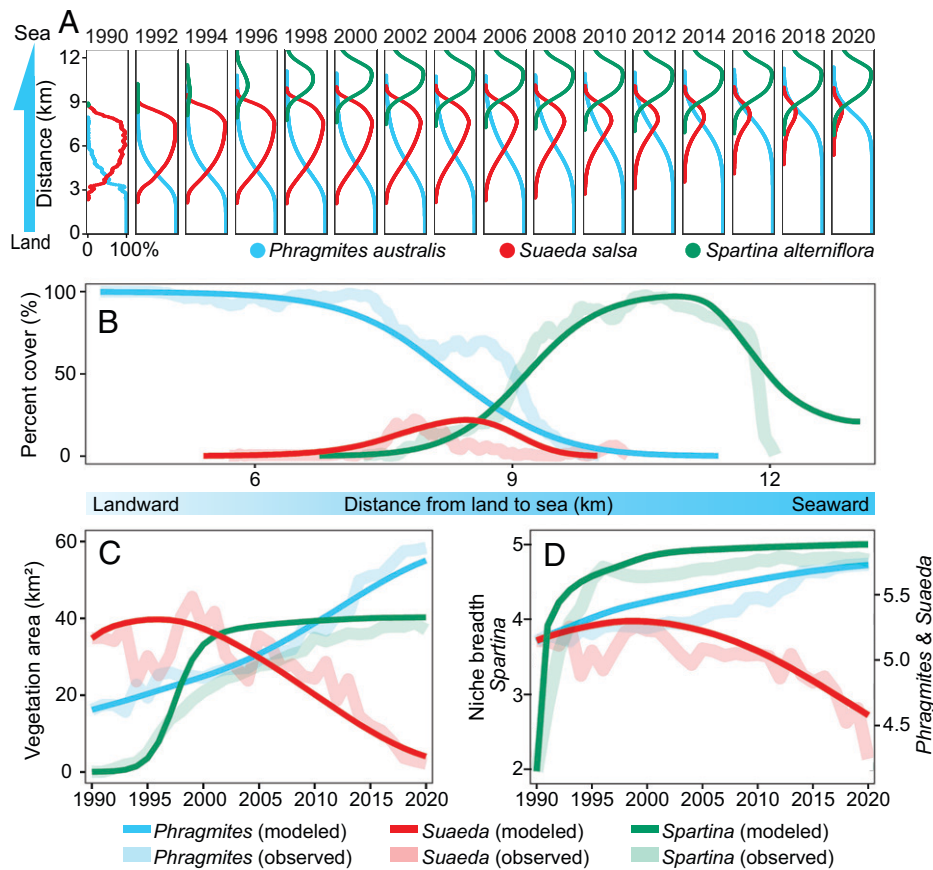
Fig. 4. Comparison between the modeled and the remotely sensed vegetation dynamics. (*A*) Modeled percent covers of vegetation (see *SI Appendix*, Fig. S2 for a complete illustration). (*B*) Modeled and observed percent vegetation covers along the land–sea spatial gradient at the end of the study time period (year 2020). (*C*) Modeled and observed (see also Fig. 3*A*) spatial extent of the three vegetation types during 1990 to 2020. (*D*) Modeled and observed (see also Fig. 3*B*) spatial niche breadths along the land–sea gradient during 1990 to 2020. See *SI Appendix*, section S1 for the methodological details.

interactions affect resilience to drought effects, mitigating drought-induced salt stress, but in parallel reduce opportunities for the recovery of *Suaeda* vegetation. Similarly, the effects of land reclamation, a critical threat to coastal ecosystem, may have unforeseen implications by interfering with long-distance effects of cordgrass (26). Our results emphasize the complexity of coastal ecosystems where both shifting environmental conditions and human activities can have a multitude of effects that link long-distance interactions to ecosystem resilience and biological invasions. Our work also paves the way for connecting local and global biotic interactions ecologically and evolutionarily. Experimental studies of intermediate spatial-scale interactions may reveal that long-distance biotic interactions, by promoting isolation by distance among sympatric species, accelerate evolutionary differentiation.

Materials and Methods

Study Area. We analyzed the landscape dynamics in the core area (114.7 km², 120°31′–120°40′ E, 33°28′–33°36′ N) of the Yancheng National Nature Reserve at the coast of the Yellow Sea, Jiangsu Province, eastern China (Fig. 1*A*). This region is dominated by a subtropical monsoon climate with a mean annual temperature of 14.9 °C and a mean annual precipitation of 1,010 mm. The study area represents an intertidal silt-muddy coastal saltmarsh landscape subject to irregular semidiurnal tides. The native saltmarshes are dominated by the perennial gramineous species *P. australis* (Fig. 1*B*) and the annual forb species *S. salsa* (Fig. 1*C*). Cordgrass *Spartina anglica* was introduced into the coastal region of Jiangsu Province in 1964 (38), but it was progressively replaced by *S. alterniflora* (Fig. 1*D*), which showed rapid expansion after 1990 (Fig. 1*E*).

Data Analyses. Vegetation distributions were mapped using the Landsat Collection 1 Tier 1 images on an annual basis from 1982 to 2020 (downloaded from the US Geological Survey EarthExplorer website, https://earthexplorer.usgs.gov/), including the Landsat MSS images for 1982 to 1983, the Landsat TM images for 1984 to 2008, the Landsat ETM+ images for 2009 to 2012, and the Landsat 8 OLI images for 2013 to 2020. The data gaps in the Landsat ETM+ images due to scan line corrector failure (SLC-off) were filled using the image composite method (39). For each year, we selected the cloud-free images acquired between October and December, because the spectral differences between the vegetation types are mostly pronounced during this low-growth season, allowing us to clearly distinguish the vegetation distributions from the remotely sensed images. We used supervised classification with the maximum likelihood method to map the spatial distribution of reeds, cordgrasses, *Suaeda* forbs, bare mudflats, and waters within the study area for each year. The results of image classification were validated using high-resolution Google Earth images and ground truth survey data. We then used the resulting classification maps to calculate the percent cover for each vegetation type on an annual basis in the study area (Fig. 3*A*).

Considering the zonation along the land–sea gradient represents the most important spatial feature of coastal ecosystem distribution, we conducted a "spatial niche" analysis to characterize how the vegetation zonation feature changed over time. To this end, we calculated the percent cover of each vegetation type on the one-dimensional space in terms of land–sea gradient. In doing so, we first split the study area into spatial transects with a width of 30 m (i.e., the resolution of the Landsat images) then calculated the proportion of each vegetation type on each transects. Percent cover was calculated for all transects (Fig. 1*F*). An intuitive interpretation is that the areas around the optima of the curves represent the cores of the "spatial niches," i.e., the core distribution ranges of the vegetation types. We used the Shannon–Weiner niche breadth index to assess the one-dimensional spatial distribution extent for each vegetation type (40) (Fig. 3*B*).
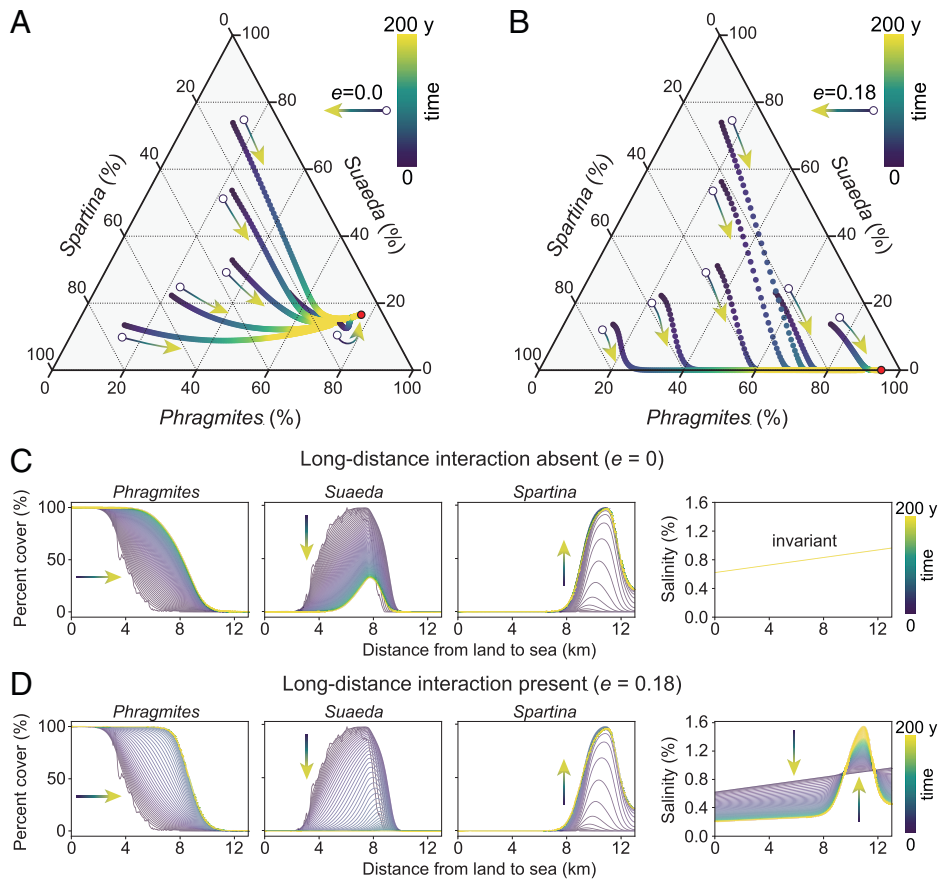
Fig. 5. Model predicted effect of long-distance interaction on system behavior. System states in terms of percent covers of the three species are illustrated using triangle plots (*A* and *B*). (*A*) In the absence of long-distance interaction (*e* = 0), the system will converge to an equilibrium characterized by the three-species coexistence (red dot). (*B*) When sufficiently strong long-distance interaction is present (*e* = 0.18), the system will converge to a two-species coexistence equilibrium at which *Suaeda* cannot be maintained. The trajectories of system state over time are shown for six randomly selected initial conditions in each scenario (*A* and *B*). (*C* and *D*) Changes of spatial patterns of the three species for the absence (*C*) and presence (*D*) of the long-distance interaction. The arrows indicate the direction of the change over time (from purple to yellow). The spatial patterns are modeled and plotted annually for 200 y. The color gradient (for the curves and arrows) from dark blue to yellow indicating modeling time from 0 to 200 y. The initial condition (*t* = 0) of vegetation cover is taken from the remotely sensed data in 1990 (the ragged curves), and the initial condition of salinity is taken from a linear fit of the measured salinity (the straight lines). The yellow curves represent steady distributions over the one-dimensional space (from land to sea). When the long-distance interaction is present, *Suaeda* cover approaches zero as an equilibrium (*D*). The spatial patterns of the steady states with different long-distance interaction strength are shown in Movie S2.

We collected the data of elevation, sediment composition, and soil salinity along the land–sea gradient within the study area from the published literature (Fig. 3 *C* and *D* and SI Appendix, Fig. S3 and Table S3). The soil salinity changes were characterized for the different vegetation zones separately (Fig. 3 *F–H*).

Spatial Model of Long-Distance Interaction. By extending the classical Lotka–Volterra model of competition, we build a one-dimensional spatial model of three-species interactions to reflect the vegetation dynamics along the coastal spatial gradient from land to sea.

In the absence of the long-distance interaction, the dynamics of species *Phragmites* (P_h, species 1), *Suaeda* (S_u, species 2), and *Spartina* (S_p, species 3) are governed by spatial diffusion and competition-mediated growth (Eqs. **1–3**):

$$\frac{\partial P_h}{\partial t} = D_1 \frac{\partial^2 P_h}{\partial x^2} + P_h\left(r(x) - a_{11}P_h - a_{21}S_u - a_{31}S_p\right) \quad \text{[1]}$$

$$\frac{\partial S_u}{\partial t} = D_2 \frac{\partial^2 S_u}{\partial x^2} + S_u\left(r(x) - a_{12}P_h - a_{22}S_u - a_{32}S_p\right) \quad \text{[2]}$$

$$\frac{\partial S_p}{\partial t} = D_3 \frac{\partial^2 S_p}{\partial x^2} + S_p\left(r(x) - a_{13}P_h - a_{23}S_u - a_{33}S_p\right), \quad \text{[3]}$$

where the percent cover of each species is modeled as a function of logistic growth (with assumed equal intrinsic growth rate *r* for different species at a given spatial location *x*), intraspecific competition (with competition coefficient a_{ii}), interspecific competition (with competition coefficient a_{ij}), and one-dimensional spatial diffusion (for plant expansion) denoted by the term $D_i \frac{\partial^2}{\partial x^2}$ (where D_i is the

diffusion coefficient for species *i*). Spatial location from land to sea and time are represented by *x* and *t*, respectively.

The invasion of cordgrass *S. alterniflora* is modeled by adding a spatial drift term $V_3 \frac{\partial S_p}{\partial x}$ (where V_3 is a directional migration coefficient of *S. alterniflora* seaward). Eq. **3** then becomes

$$\frac{\partial S_p}{\partial t} = D_3 \frac{\partial^2 S_p}{\partial x^2} + S_p\left(r(x) - a_{13}P_h - a_{23}S_u - a_{33}S_p\right) - V_3\frac{\partial S_p}{\partial x}. \quad \text{[4]}$$

The influence of (tidal) sea water on intrinsic growth rate *r(x)* is modeled as linear decline with distance to the sea. Within the zone of influence (i.e., when $L_s - w \le x \le L_s$), $r(x) = (L_s - x)/w$, where L_s is the location of permanent sea water (i.e., shoreline at low tides), and *w* is the spatial extent at which vegetation growth is influenced by sea water. Outside the zone of influence, $r(x) = 0$ when $x > L_s$ (permanently under sea water), and $r(x) = 1.0$ when $x < L_s - w$ (high elevations).

Long-distance interaction through mediating soil salinity (S_a) is a key mechanism that possibly makes the system substantially go beyond the competition-mediated dynamics. We consider two competing processes that influence salinity, i.e., salt input from tidal water vs. salt loss (desalination) through surface and sub-surface flow. The effects of cordgrass growth on these two processes are modeled as

$$\frac{\partial S_a}{\partial t} = (c - S_a)f + d\frac{S_p}{b + S_p}S_a - \frac{eS_a}{|\Omega|}\int_\Omega S_p(x)dx. \quad \text{[5]}$$

The first term $(c - S_a)f$ describes the supplement of soil salinity through sea water, where constant *c* and *f* represent the salt input rate of sea water and salt
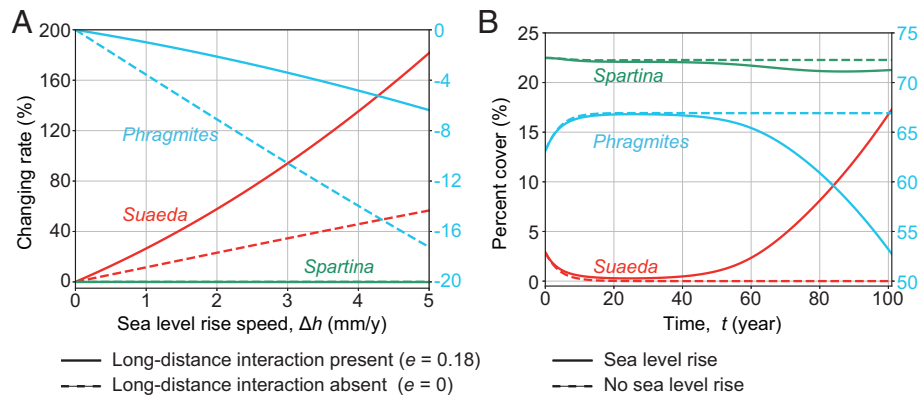
Fig. 6. Model-predicted effect of long-distance interaction on coastal resilience. (*A*) The model predicts increasing growths of *Suaeda* as well as declines of *Phragmites* with increasing speed of sea-level rise. The presence of the long-distance interaction (solid lines) can result in amplified growth rates of *Suaeda* and the reduced loss rate of *Phragmites*, as compared with the situation absent of the long-distance interaction (dashed lines). The model thus predicts higher resilience of the coastal ecosystems (in terms of persistence of the native *Suaeda* and *Phragmites* vegetation) facing sea-level rise. (*B*) In the presence of long-distance interaction, *Suaeda* is predicted to increase whereas *Phragmites* and *Spartina* are predicted to decline in the upcoming ~40 y with accelerated sea-level rise (solid lines) at a speed of 5.0 mm per year (~50% increase over the current speed). Note that in each panel the *y* axis at the right-hand side (with blue labels) indicates *Phragmites*.

exchange rate between sea water and soil, respectively. The second term $d\frac{S_p}{b+S_p}S_a$ represents a local salt enrichment effect through cordgrass growth, where the constant d is the enrichment coefficient, and $\frac{S_p}{b+S_p}$ is used to model the saturation trend of the enrichment effect. The third term $\frac{eS_a}{|\Omega|}\int_\Omega S_p(x)dx$ represents desalination effect of cordgrass growth on the rear tidal flat (through reducing tide inundation as a result of increasing elevation in the low-tide zone). This desalination process can occur at long distances from the locations of cordgrasses. The coefficient e of this desalination effect thus reflects the strength of the long-distance interaction.

We model the effect of soil salinity on the species interaction by integrating a salinity-dependent competition coefficient into the dynamics of *Suaeda*. That is, in Eq. **2** we replace a_{12} with $\frac{a_{12}}{S_a+a}$, where changes of soil salinity are assumed to affect the competition coefficient of *Suaeda* against *Phragmites*. As *Phragmites* is less salt-tolerant than *Suaeda*, decreasing salinity can facilitate *Phragmites* competing with *Suaeda*. a is a half-saturation constant. Eq. **2** now becomes

$$\frac{\partial S_u}{\partial t} = D_2\frac{\partial^2 S_u}{\partial x^2} + S_u\left(r(x) - \frac{a_{12}}{S_a+a}P_h - a_{22}S_u - a_{32}S_p\right). \quad [6]$$

We use the model (given by Eqs. **1**, **4**, **5**, and **6**) to investigate the role of long-distance interaction (by changing the parameter e) in driving vegetation dynamics. We further infer how the system may respond to sea-level rise and perturbations, which are considered key challenges of coastal ecosystems (41). The effect

of sea-level rise is modeled by changing salt input rate c. Parameter definitions and default values are given in *SI Appendix*, Table S1.

Data Availability. All codes are available online at the GitHub repository: https://github.com/liuqx315/B.Wang-et-al-PNAS-2022 (42). All other study data are included in the article and/or supporting information.

Author affiliations: [a]School of Life Sciences, Nanjing University, Nanjing 210023, China; [b]Center for Global Change and Complex Ecosystems, School of Ecological and Environmental Sciences, East China Normal University, Shanghai 200241, China; [c]State Key Laboratory of Estuarine and Coastal Research, East China Normal University, Shanghai 200241, China; [d]Coastal Ecology Lab, National Observation and Research Station for Shanghai Yangtze Estuarine Wetland Ecosystems, Ministry of Education Key Laboratory for Biodiversity Science and Ecological Engineering, School of Life Sciences, Fudan University, Shanghai 200438, China; [e]Royal Netherlands Institute for Sea Research, 4400 AC Yerseke, The Netherlands; [f]Groningen Institute for Evolutionary Life Sciences, University of Groningen, 9700 CC Groningen, The Netherlands; and [g]Department of Ecology, Evolution and Organismal Biology, Brown University, Providence, RI 02912

1. G. E. Hutchinson, Homage to Santa Rosalia or why are there so many kinds of animals? *Am. Nat.* **93**, 145–159 (1959).
2. E. Andresen, V. Arroyo-Rodríguez, F. Escobar, "Tropical biodiversity: The importance of biotic interactions for its origin, maintenance, function, and conservation" in *Ecological Networks in the Tropics*, W. Dáttilo, V. Rico-Gray, Eds. (Springer, 2018), pp. 1–13.
3. J. H. Brown, Two decades of homage to Santa Rosalia: Toward a general theory of diversity. *Am. Zool.* **21**, 877–888 (1981).
4. M. Vellend, *The Theory of Ecological Communities (MPB-57)* (Princeton University Press, 2016).
5. J. Olejarz, Y. Iwasa, A. H. Knoll, M. A. Nowak, The Great Oxygenation Event as a consequence of ecological dynamics modulated by planetary change. *Nat. Commun.* **12**, 3985 (2021).
6. C. A. Klausmeier, Regular and irregular patterns in semiarid vegetation. *Science* **284**, 1826–1828 (1999).
7. M. Rietkerk *et al.*, Self-organization of vegetation in arid ecosystems. *Am. Nat.* **160**, 524–530 (2002).
8. J. F. Bruno, Facilitation of cobble beach plant communities through habitat modification by *Spartina alterniflora*. *Ecology* **81**, 1179–1192 (2000).
9. J. van de Koppel *et al.*, Long-distance interactions regulate the structure and resilience of coastal ecosystems. *Annu. Rev. Mar. Sci.* **7**, 139–158 (2015).
10. S. Donadi *et al.*, Cross-habitat interactions among bivalve species control community structure on intertidal flats. *Ecology* **94**, 489–498 (2013).
11. J. van de Koppel, A. H. Altieri, B. R. Silliman, J. F. Bruno, M. D. Bertness, Scale-dependent interactions and community structure on cobble beaches. *Ecol. Lett.* **9**, 45–50 (2006).
12. Q.-X. Liu *et al.*, Phase separation explains a new class of self-organized spatial patterns in ecological systems. *Proc. Natl. Acad. Sci. U.S.A.* **110**, 11905–11910 (2013).
13. M. Rietkerk, J. van de Koppel, Regular pattern formation in real ecosystems. *Trends Ecol. Evol.* **23**, 169–175 (2008).
14. M. Rietkerk *et al.*, Evasion of tipping in complex systems through spatial pattern formation. *Science* **374**, eabj0359 (2021).
15. M. Loreau, N. Mouquet, R. D. Holt, Meta-ecosystems: A theoretical framework for a spatial ecosystem ecology. *Ecol. Lett.* **6**, 673–679 (2003).
16. E. Benincà, B. Ballantine, S. P. Ellner, J. Huisman, Species fluctuations sustained by a cyclic succession at the edge of chaos. *Proc. Natl. Acad. Sci. U.S.A.* **112**, 6389–6394 (2015).
17. E. C. Shaver, B. R. Silliman, Time to cash in on positive interactions for coral restoration. *PeerJ* **5**, e3499 (2017).
18. S. R. Valdez *et al.*, Positive ecological interactions and the success of seagrass restoration. *Front. Mar. Sci.* **7**, 91 (2020).
19. F. Shi *et al.*, Toward an ecological civilization: Mass comprehensive ecotourism indications among domestic visitors to a Chinese wetland protected area. *Tour. Manage.* **70**, 59–68 (2019).
20. S. Gao *et al.*, Environment-ecosystem dynamic processes of *Spartina alterniflora* salt-marshes along the eastern China coastlines. *Sci. China Earth Sci.* **57**, 2567–2586 (2014).
21. C. Wang *et al.*, Diverse usage of waterbird habitats and spatial management in Yancheng coastal wetlands. *Ecol. Indic.* **117**, 106583 (2020).
22. C. E. Studds *et al.*, Rapid population decline in migratory shorebirds relying on Yellow Sea tidal mudflats as stopover sites. *Nat. Commun.* **8**, 14895 (2017).
23. Z. Ma, Z. Wang, H. Tang, Habitat use and selection by Red-crowned Crane *Grus japonensis* in winter in Yancheng Biosphere Reserve, China. *Ibis* **141**, 135–139 (1999).
24. N. Li *et al.*, Effects of long-term coastal reclamation on suitable habitat and wintering population size of the endangered Red-crowned Crane, *Grus japonensis*. *Hydrobiologia* **827**, 21–29 (2019).
25. L. Cui *et al.*, *Phragmites australis* meets *Suaeda salsa* on the "red beach": Effects of an ecosystem engineer on salt-marsh litter decomposition. *Sci. Total Environ.* **693**, 133477 (2019).
26. J. Ren *et al.*, An invasive species erodes the performance of coastal wetland protected areas. *Sci. Adv.* **7**, eabi8943 (2021).
27. A. C. Redfield, Development of a New England salt marsh. *Ecol. Monogr.* **42**, 201–237 (1972).
28. M. G. Hughes, K. Rogers, L. Wen, Saline wetland extents and tidal inundation regimes on a micro-tidal coast, New South Wales, Australia. *Estuar. Coast. Shelf Sci.* **227**, 106297 (2019).

29. Y.-H. Wang *et al.*, Development and mechanism of transitional coast. *Ocean Eng.* **21**, 65–70 (2003) (in Chinese).

30. X.-Y. Liu, J.-H. Gao, F.-L. Bai, Z.-Y. Liu, S.-M. Pan, Grain size information in different evolution periods of Xinyanggang tidal flat in Jiangsu Province. *Mar. Geol. Q. Geol.* **28**, 27–35 (2008) (in Chinese).

31. Y. Zhao *et al.*, Rapid formation of marsh-edge cliffs, Jiangsu coast, China. *Mar. Geol.* **385**, 260–273 (2017).

32. M. D. Bertness, A. M. Ellison, Determinants of pattern in a New England salt marsh plant community. *Ecol. Monogr.* **57**, 129–147 (1987).

33. S. C. Pennings, R. M. Callaway, Salt marsh plant zonation: The relative importance of competition and physical factors. *Ecology* **73**, 681–690 (1992).

34. A. C. Ross *et al.*, Sea-level rise and other influences on decadal-scale salinity variability in a coastal plain estuary. *Estuar. Coast. Shelf Sci.* **157**, 79–92 (2015).

35. J. van de Koppel, D. van der Wal, J. P. Bakker, P. M. J. Herman, Self-organization and vegetation collapse in salt marsh ecosystems. *Am. Nat.* **165**, E1–E12 (2005).

36. M. Rietkerk, S. C. Dekker, P. C. de Ruiter, J. van de Koppel, Self-organized patchiness and catastrophic shifts in ecosystems. *Science* **305**, 1926–1929 (2004).

37. M. Bertness, *A Brief Natural History of Civilization: Why a Balance Between Cooperation & Competition is Vital to Humanity* (Yale University Press, 2020).

38. C.-H. Chung, Thirty years of ecological engineering with *Spartina* plantations in China. *Ecol. Eng.* **2**, 261–289 (1993).

39. P. Scaramuzza, E. Micijevic, G. Chander, "SLC gap-filled products phase one methodology" (Landsat Tech. Notes 5, US Geological Survey, 2004).

40. A. E. Magurran, *Ecological Diversity and Its Measurement* (Princeton University Press, 1988).

41. Q. He, B. R. Silliman, Climate change, human impacts, and coastal ecosystems in the Anthropocene. *Curr. Biol.* **29**, R1021–R1035 (2019).

42. B. Wang *et al.*, Data from "Long-distance facilitation of coastal ecosystem structure and resilience." GitHub. https://github.com/liuqx315/B.Wang-et-al-PNAS-2022. Deposited 5 June 2022.